ChemComm

COMMUNICATION

View Article Online
View Journal | View Issue

Cite this: *Chem. Commun.*, 2023, 59, 3087

Received 21st December 2022,
Accepted 14th February 2023

DOI: 10.1039/d2cc06950d

rsc.li/chemcomm

Ginsenoside Rg_1 modulates vesicular dopamine storage and release during exocytosis revealed with single-vesicle electrochemistry†

Junlan Zhou,‡[ab] Jing Zhang,‡[ab] Lijiao Cao,[ab] Yuying Liu,[abc] Luyao Liu,[ab] Chunlan Liu*[ab] and Xianchan Li *[abc]

Ginsenoside Rg_1, a tetracyclic triterpenoid derivative extracted from the roots of *Panax ginseng* C. A. Meyer, can enhance learning and memory and improve cognitive impairment. However, whether or how it affects vesicular dopamine storage and its release during exocytosis remains unknown. By using single-vesicle electrochemistry, we for the first time find out that Rg_1 not only upregulates vesicular dopamine content but also increases exocytosis frequency and modulates dopamine release during exocytosis in PC12 cells, which may relate to the activation of protein kinases, causing a series of biological cascades. This finding offers the possible link between Rg_1 and vesicular chemical storage and exocytotic release, which is of significance for understanding the nootropic role of Rg_1 from the perspective of neurotransmission.

Ginsenoside Rg_1 (structure shown in Fig. 1a) is a tetracyclic triterpenoid derivative extracted from the roots of *Panax ginseng* C. A. Meyer. This compound exhibits diverse bioactivities, including neurogenesis promotion, anti-aging, anti-fatigue, immunity enhancement, and adjuvant anti-tumor effect.[1] As a small molecule, ginsenoside Rg_1 can cross the blood-brain barrier and affect various molecules, such as growth factors, adenosine triphosphate (ATP), and different enzymes, thereby regulating signalling pathways in the brain.[2] Recent studies have shown that ginsenoside Rg_1 can improve cognitive impairment by inducing long-time potentiation, improving synaptic plasticity, increasing neurogenesis, and inhibiting neuronal apoptosis.[3] This implies that ginsenoside Rg_1 may be a potential drug for neurodegenerative diseases.[1] Growing evidence proves that cognitive impairment in neurodegenerative diseases is inextricably linked to neurotransmitter disorders in the brain.[4–6] However, whether and how ginsenoside Rg_1 affects neurotransmitter storage and release in the nervous system is still unknown.

It is known that exocytosis of neurotransmitters occurs at the nanometer spatial scale and millisecond time scale. Therefore, a high spatiotemporal resolution approach is required to quantitatively monitor the dynamics of neurotransmitter storage and release in real-time. Single-vesicle electrochemistry, including the single cell amperometry (SCA)[7–11] and intracellular vesicle impact electrochemical cytometry (IVIEC),[12–14] have been developed to monitor the neurotransmitter release during exocytosis and quantify the neurotransmitter content in single vesicles in living cells, respectively. Growing evidence proves the coupling of SCA and IVIEC can provide more information on neurotransmitter metabolism and transportation in the nervous system and help us understand neurotransmission.[12,15–19]

The exploration of whether and how ginsenoside Rg_1 acts on neurotransmitter storage and release will largely contribute to our understanding of its neuroprotective effects at the single vesicle level. In this study, we used rat pheochromocytoma (PC12) cells, a kind of neuroendocrine cell, as a model cell to

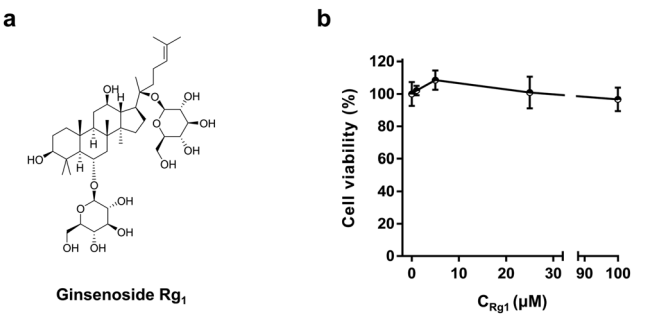

Fig. 1 Chemical structure of ginsenoside Rg_1 (a) and MTT assay for PC12 cells treated with 1, 5, 25, and 100 μM Rg_1 for 3 h (b).

[a] *Key Laboratory of Mass Spectrometry Imaging and Metabolomics (Minzu University of China), National Ethnic Affairs Commission, Beijing 100081, China. E-mail: xcli@hsc.pku.edu.cn, liuchunlan@muc.edu.cn*
[b] *Center for Imaging and Systems Biology, College of Life and Environmental Sciences, Minzu University of China, Beijing 100081, China*
[c] *State Key Laboratory of Natural and Biomimetic Drugs and Department of Pharmaceutical Analysis, School of Pharmaceutical Sciences, Peking University, Beijing 100191, China*

† Electronic supplementary information (ESI) available. See DOI: https://doi.org/10.1039/d2cc06950d

‡ Junlan Zhou and Jing Zhang contributed equally.

investigate the effect of Rg_1 on neurotransmitter storage and release.

Ginsenoside Rg_1 has been reported to suppress the proliferation of tumor cells. To test the effect of Rg_1 on PC12 cells, the MTT cell viability assay was taken to examine the cell viability over a concentration range of Rg_1.[12,15] As shown in Fig. 1b, in the concentration range of 1–100 μM,[20] the cell viability did not change significantly upon Rg_1 treatment for 3 h although 5 μM Rg_1 seems to slightly increase the PC12 cell viability. In the following study, 25 μM Rg_1 was used.[21]

IVIEC using nano-tip conical electrodes (Fig. 2a, b and Fig. S1a, ESI†) was used to quantify the vesicular dopamine content of PC12 cells.[12,13] Representative *i–t* traces obtained from the amperometric recording of vesicular dopamine storage in PC12 cells are displayed in Fig. 2c. Each amperometric spike in the *i–t* trace represents the electrooxidation of dopamine in one vesicle to dopamine-quinone at the nano-tip conical electrode surface. Typical spikes showing the single events of Rg_1-treated and untreated PC12 cells are shown in Fig. 2d.

Fig. 2e compares the normalized frequency histogram of the dopamine content in single vesicles ($N_{storage}$) in Rg_1-treated PC12 cells and control cells. Obviously, $N_{storage}$ of Rg_1-treated PC12 cells is much higher than control cells. Further statistical analysis (Fig. 2f) proves a significant difference between two groups (*i.e.* $(8.76 \pm 0.73) \times 10^4$ for control, $(11.25 \pm 0.84) \times 10^4$ for 25 μM Rg_1 treatment). It reveals that 25 μM Rg_1 treatment significantly upregulates the vesicular dopamine storage in PC12 cells. This might relate to the upregulation of tyrosine hydroxylase activity by the protein kinase, in turn promoting dopamine synthesis in cytosol (*vide infra*).[22]

We then used SCA with a disk carbon fiber microelectrode to investigate the effect of 25 μM Rg_1 on neurotransmitter release during exocytosis (Fig. 3a, b and Fig. S1b, ESI†). Due to its high

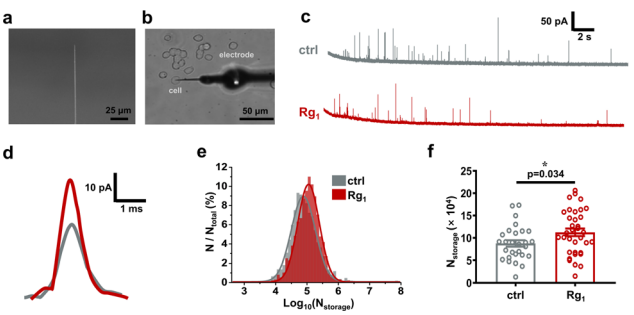

Fig. 2 Electrochemical quantification of vesicular dopamine content in PC12 cells by IVIEC. (a) Scan electron microscopy (SEM) of a nano-tip conical carbon fiber electrode. Scale bar, 25 μm. (b) Bright-field photomicrograph of the experimental setup of IVIEC with a nano-tip electrode. Scale bar, 50 μm. Typical IVIEC traces (c) and amperometric spikes (d) of PC12 cells treated without (grey) or with (red) 25 μM Rg_1. (e) Normalized frequency histogram of log of the vesicular dopamine amount of control (grey, 1107 spikes from 30 cells) and Rg_1-treated group (red, 1365 peaks from 35 cells). Fits were obtained with a Gaussian distribution of the data. (f) Plots describing the average vesicular dopamine amounts measured with IVIEC. Error bar, standard error of the mean (SEM). The data sets were compared using a Wilcoxon–Mann–Whitney test. *, $p < 0.05$.

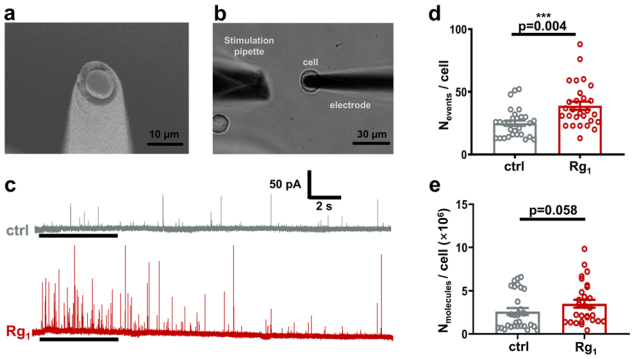

Fig. 3 Electrochemical quantification of vesicular dopamine released during exocytosis from PC12 cells by SCA. (a) SEM image of a disk carbon fiber electrode. Scale bar, 10 μm. (b) Bright-field photomicrograph of SCA experimental setup with a disk electrode. Scale bar, 30 μm. (c)Typical SCA traces of PC12 cells treated without (grey) or with (red) 25 μM Rg_1 for 3 h. The black lines indicate the 5-s stimulation with 70 mM K^+. The number of events recorded (d) and the number of cumulative dopamine molecules released (e) per PC12 cell treated without or with 25 μM Rg_1 upon once high K^+ stimulation. Error bar, SEM. The pairs of data sets were compared using a Wilcoxon–Mann–Whitney test. ***, $p < 0.001$.

sensitivity and high spatial-temporal resolution, SCA has successfully been used to quantify neurotransmitter released during exocytosis and monitor the kinetics of exocytosis in various cell models.[23]

While stimulating with 70 mM K^+ solution, a train of amperometric spikes was obtained (Fig. 3c). Different from the IVIEC, each amperometric spike in SCA traces represents the electrooxidation of dopamine released during an exocytotic event to dopamine-quinone. Apparently, 25 μM Rg_1 treatment stimulates the dopamine release by increasing both the number of exocytotic events and the spike current. As shown in Fig. 3d, the statistical comparison displays significant increase of the number of exocytotic events per cell (N_{events}/cell) by Rg_1 treatment (*i.e.* 39 ± 3 for Rg_1-treated group, 25 ± 2 for control group, $p = 0.004$), indicating Rg_1 treatment elevates exocytotic frequency. To investigate if Rg_1 elevates dopamine amount released from single cells, we cumulated the amount of dopamine molecule released in each PC12 cell upon once high K^+ stimulation ($N_{molecules}$/cell). Although not significantly, $N_{molecules}$ per cell in Rg_1 group is slightly higher than control group (*i.e.*, $(3.51 \pm 0.46) \times 10^6$ molecules for Rg_1 group *vs.* $(2.60 \pm 0.41) \times 10^6$ molecules for control group). The elevation of exocytosis frequency and dopamine release may be relevant to the enhancement of Ca^{2+} influx by Rg_1 (*vide infra*).

It has been reported that amperometric spikes parameters demonstrate several vital processes of exocytosis (Fig. 4a).[24] To further explore the effect of Rg_1 on cell exocytosis, we compared the exocytotic spike parameters obtained from control cells and Rg_1-treated cells (Fig. 4b–j and Fig. S2 and S3, ESI†).

As shown in Fig. 4c and Fig. S2d (ESI†), I_{max} of Rg_1-treated cells (*i.e.* 17.20 ± 1.28 pA) is higher than the untreated cells (*i.e.* 12.29 ± 0.58 pA) significantly, suggesting that the size of fusion pore of Rg_1-treated cells is larger than the control group. Meanwhile, a noteworthy decrease of $t_{1/2}$ in Rg_1-treated cells

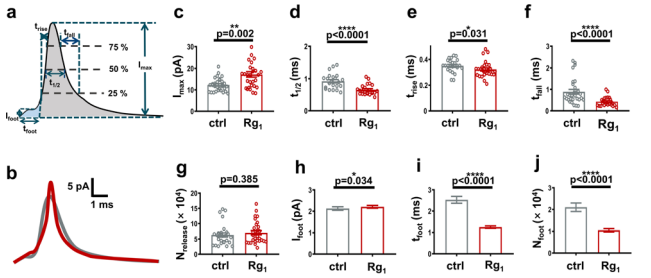

Fig. 4 Spike and pre-spike analysis of dopamine release during exocytosis from PC12 cells. (a) Scheme showing the parameters used for peak analysis. (b) Typical spikes of the cells treated without (grey) and with (red) 25 μM Rg_1. Comparison of I_{max} (c), $t_{1/2}$ (d), t_{rise} (e), t_{fall} (f), and $N_{release}$ (g) of exocytotic spikes. Control group (grey, 799 spikes from 30 cells), Rg_1 group (red, 1441 spikes from 30 cells). Comparison of I_{foot} (h), t_{foot} (i), and N_{foot} (j) of exocytotic pre-spikes (I_{foot} > 1 pA). Control group (grey, 297 spikes), Rg_1 group (red, 431 spikes). Error bar, SEM. The pairs of data sets were compared using a Wilcoxon–Mann–Whitney test, and p is indicated next to the variation. *, $p < 0.05$; **, $p < 0.01$; ****, $p < 0.0001$.

(*i.e.* 0.65 ± 0.03 ms for Rg_1-treated cells *vs.* 0.92 ± 0.05 ms for control group) was observed as depicted in Fig. 4d and Fig. S2a (ESI†), revealing that Rg_1 treatment virtually affects the exocytosis kinetics besides fusion pore size. The adverse effects of Rg_1 on I_{max} and $t_{1/2}$ lead to no obvious change on dopamine number released in single exocytotic event (Fig. 4g and Fig. S2e (ESI†), $N_{release}$, (7.07 ± 0.68) × 10^4 for Rg_1-treated *vs.* (6.33 ± 0.68) × 10^4 for control cells). This indicates Rg_1 treatment does not affect the neurotransmitter amount released by single vesicles during exocytosis.

Besides $t_{1/2}$, the duration of exocytosis could be demonstrated with t_{rise} and t_{fall}, the opening and closing time of the fusion pore, respectively.[24] As shown in Fig. 4e and Fig. S2b (ESI†), there is a slightly significant decrease of t_{rise} in the Rg_1 treatment group compared with control (*i.e.* 0.32 ± 0.01 ms for Rg_1-treated cells *vs.* 0.35 ± 0.01 ms for untreated cells, p = 0.031), suggesting that the enlarging time of fusion pore gets shorten after Rg_1 treatment. Further analysis of pre-spike foot (schemed in Fig. 4a) has been widely used to study the geometry and stability of the initial fusion pore of exocytosis. As same as the trend of t_{rise}, Fig. 4i shows that Rg_1 treatment significantly decreases the duration of foot (t_{foot}). Subsequently, it decreases the number of dopamine released *via* the initial fusion pore (Fig. 4j). These results suggest that Rg_1 treatment accelerates the forming of the initial fusion pore and the enlarging of fusion pore.

Next, we analyzed the closing time of the fusion pore (*i.e.* t_{fall}). As demonstrated in Fig. 4f, there is a significant reduction of t_{fall} after Rg_1-treatment compared with control cells (*i.e.* 0.46 ± 0.04 ms for Rg_1 group *vs.* 0.89 ± 0.10 ms for control, $p < 0.0001$). To provide more insights into the shortened decay time (t_{fall}) induced by Rg_1 treatment, further mathematical analysis was carried out. Previously studies have shown that the decay phase of exocytic amperometric peaks can be fitted with either single exponential or double exponential.[15,25] In the full fusion mode, exocytosis is largely controlled by the pure diffusion of the neurotransmitter through the fusion pore, thus its descent fraction can be well fitted with single exponential. Reversely, vesicle releases only a portion of neurotransmitters before the fusion pore closes in the partial release mode, in which the fusion pore's contraction must be faster than the neurotransmitter diffusion from the vesicle. Therefore, in the partial release mode of exocytosis, the decaying phase of exocytotic peaks is more appropriate to fit with double exponential. According to the previously published mathematical model,[26] we fitted the descent fraction of all peaks with double exponential (eqn (S1), ESI†) and obtained T_1 and T_2, which are associated with the pore contraction and neurotransmitter diffusion, respectively.

The standardized d values were calculated according to eqn (S2) and Fig. S4a (ESI†). The spikes with $d > 0.5$ were previously considered more suitable for double exponential fitting.[26] Fig. S4b (ESI†) shows that Rg_1 treatment shifts the curve to the left ($n_{d>0.5}/n_{d<0.5}$ = 651/787 for Rg_1 group *vs.* $n_{d>0.5}/n_{d<0.5}$ = 330/468 for control group). This means the number of spikes with $d > 0.5$ slightly increases after Rg_1 treatment (shown in Fig. S4c (ESI†), 45.3% for Rg_1 group *vs.* 41.4% for control, when d = 0.5). This result suggests that Rg_1 treatment promotes the collapse of fusion pores and more vesicles tend to secrete with the partial release mode. This finding is consistent with the phenomenon that a slightly lower percentage of vesicular dopamine is released during exocytosis in PC12 cells treated with Rg_1 (62.8%) than that from the control group (72.3%) when comparing the results shown in Fig. 2f with Fig. 4g.

Generally, secretory vesicles are categorized into two types: one is small synaptic vesicles (SSVs, ~50 nm in diameter), and the other is large dense core vesicles (LDCVs, 50–300 nm in diameter), to which most vesicles in PC12 cells belong. Except the difference in size and distribution, LDCVs consist of a dense core and a lucent solution called halo. The dense core, which is composed of an assortment of soluble materials inward, can reduce the osmolality of the vesicle, giving the green light for loading a high concentration of transmitters into vesicles.[27,28] Once the volume of the dense core or halo changes, the vesicular neurotransmitter concentration changes together.[29] To investigate the influence of vesicle size by Rg_1 treatment, transmission electron microscopy (TEM) imaging was performed. As depicted in Fig. S5 (ESI†), neither size of vesicle nor its compartments, including the dense core and halo changes significantly by Rg_1 treatment. Therefore, the influence of vesicular dopamine storage and release caused by Rg_1 treatment is irrelevant to the vesicle size.

Ginsenoside Rg_1 may influence neurotransmission through two signalling pathways. One is probably the direct hindrance of phosphodiesterase (PDE) activity by Rg_1, which would upregulate the concentration of intracellular cAMP, activating protein kinase A (PKA).[30] And the other may be related to the upregulating the concentration of extracellular glutamate which could elevate calcium internal stream *via* oblique activation of intracellular *N*-Methyl-D-aspartic acid (NMDA) receptors.[31,32] As depicted in Fig. S6 (ESI†), a higher calcium influx is observed following 25 μM Rg_1 treatment, confirming that Rg_1 could boot calcium influx, which tends to facilitate the

occurrence of exocytosis (Fig. 3d). And the elevated intracellular Ca^{2+} appears to activate phospholipase C-protein kinase C (PLC-PKC) pathway and calmodulin-dependent protein kinase (CaMK II).[33]

Together with PKA activated through another pathway, PKC and CaMK II might phosphorylate tyrosine hydroxylase and SNARE proteins and other proteins or enzymes. The phosphorylation of tyrosine hydroxylase could elevate the synthesis of dopamine,[22] thus promoting dopamine storage in single vesicles (Fig. 2f). The formation of SNAREs complex is the core leading to membrane fusion in exocytosis. Once any change of the SNAREs protein occurs, it may have a dramatic impact on extracellular secretion. It has been reported that PKC could phosphorylate syntaxin and/or SNAP-25, attenuating their adhesion with synaptobrevin,[34] and thus shorten the opening and closing time of the exocytotic fusion pore, through which less fraction of transmitter released (Fig. S7, ESI†).

In conclusion, by using single-vesicle electrochemistry, we investigate the influence of ginsenoside Rg_1 on vesicular transmitter storage and its release during exocytosis. Our results show that the Rg_1 treatment up-regulates the dopamine content in single vesicles. Besides, Rg_1 can significantly increase the exocytosis frequency of PC12 cells, which may be related to the promotion of Ca^{2+} influx by Rg_1. Moreover, Rg_1 significantly shortens the duration time of exocytosis, including the opening and closing time of exocytotic fusion pores. Further analysis suggests that Rg_1 not only affects the fusion pore at the initial forming stage and its enlarging process, but also promotes the collapse of the fusion pore, which may correlate with the activation of CaMK II, PKA, and PKC, subsequently phosphorylating SNAREs proteins. Taking the different aspects from the current study of Rg_1 effect on transmitter synthesis, storage and release during exocytosis, our results are helpful for better understanding the nootropic effect of Rg_1 from the perspective of neurotransmission.

The authors are grateful for the financial support from the National Key Research and Development Program of China (2022YFA1200067), the National Natural Science Foundation of China (21974154), Recruitment Program of Global Experts (Youth).

Conflicts of interest

There are no conflicts to declare.

Notes and references

1 A. Rajabian, M. Rameshrad and H. Hosseinzadeh, *Expert Opin. Ther. Pat.*, 2019, **29**, 55–72.
2 T. Huang, F. Fang, L. Chen, Y. Zhu, J. Zhang, X. Chen and S. S. Yan, *Curr. Alzheimer Res.*, 2012, **9**, 388–395.
3 F. Li, X. Wu, J. Li and Q. Niu, *Mol. Med. Rep.*, 2016, **13**, 4904–4910.
4 R. I. Teleanu, A. G. Niculescu, E. Roza, O. Vladâcenco, A. M. Grumezescu and D. M. Teleanu, *Int. J. Mol. Sci.*, 2022, **23**, 5954.
5 C. Xu, Y. Jiang, P. Yu and L. Mao, *Int. J. Electrochem.*, 2022, **28**, 2108551.
6 L. Shi, M. Liu, L. Zhang and Y. Tian, *Angew. Chem., Int. Ed.*, 2022, **61**, e202117125.
7 B. B. Anderson, S. E. Zerby and A. G. Ewing, *J. Neurosci. Methods*, 1999, **88**, 163–170.
8 R. M. Wightman, J. A. Jankowski, R. T. Kennedy, K. T. Kawagoe, T. J. Schroeder, D. J. Leszczyszyn, J. A. Near, E. J. Diliberto Jr and O. H. Viveros, *Proc. Natl. Acad. Sci. U. S. A.*, 1991, **88**, 10754–10758.
9 K. Wang, X. Zhao, B. Li, K. Wang, X. Zhang, L. Mao, A. Ewing and Y. Lin, *Anal. Chem.*, 2017, **89**, 8683–8688.
10 C. Gu, X. Zhang and A. G. Ewing, *Anal. Chem.*, 2020, **92**, 10268–10273.
11 L. Ren, A. Oleinick, I. Svir, C. Amatore and A. G. Ewing, *Angew. Chem., Int. Ed.*, 2020, **59**, 3083–3087.
12 X. Li, J. Dunevall and A. G. Ewing, *Angew. Chem., Int. Ed.*, 2016, **55**, 9041–9044.
13 X. Li, S. Majdi, J. Dunevall, H. Fathali and A. G. Ewing, *Angew. Chem., Int. Ed.*, 2015, **54**, 11978–11982.
14 J. G. Roberts, E. C. Mitchell, L. E. Dunaway, G. S. McCarty and L. A. Sombers, *ACS Nano*, 2020, **14**, 2917–2926.
15 X. Li, A. S. Mohammadi and A. G. Ewing, *J. Electroanal. Chem.*, 2016, **781**, 30–35.
16 X. He and A. G. Ewing, *Chem. Sci.*, 2022, **13**, 1815–1822.
17 Q. Yue, X. Li, F. Wu, W. Ji, Y. Zhang, P. Yu, M. Zhang, W. Ma, M. Wang and L. Mao, *Angew. Chem., Int. Ed.*, 2020, **59**, 11061–11065.
18 Q. Yue, K. Wang, M. Guan, Z. Zhao, X. Li, P. Yu and L. Mao, *Angew. Chem., Int. Ed.*, 2022, **61**, e202117596.
19 Y. Liu, J. Du, M. Wang, J. Zhang, C. Liu and X. Li, *Front. Chem.*, 2021, **8**, 591311.
20 J. Wang, J. Hou, H. Lei, J. Fu, Y. Pan and J. Liu, *Mol. Med. Rep.*, 2015, **12**, 5328–5334.
21 H. Miao, Y. Zhen, G. Ding, F. Hong, Z. Xie and M. Tian, *Biomed. Environ. Sci.*, 2015, **28**, 116–126.
22 K. A. Albert, E. Helmer-Matyjek, A. C. Nairn, T. H. Müller, J. W. Haycock, L. A. Greene, M. Goldstein and P. Greengard, *Proc. Natl. Acad. Sci. U.S.A.*, 1984, **81**, 7713–7717.
23 A. Larsson, S. Majdi, A. Oleinick, I. Svir, J. Dunevall, C. Amatore and A. G. Ewing, *Angew. Chem., Int. Ed.*, 2020, **59**, 6711–6714.
24 E. V. Mosharov and D. Sulzer, *Nat. Methods*, 2005, **2**, 651–658.
25 C. T. Wang, R. Grishanin, C. A. Earles, P. Y. Chang, T. F. Martin, E. R. Chapman and M. B. Jackson, *Science*, 2001, **294**, 1111–1115.
26 R. Trouillon and A. G. Ewing, *ACS Chem. Biol.*, 2014, **9**, 812–820.
27 X. Li, J. Dunevall and A. G. Ewing, *Acc. Chem. Res.*, 2016, **49**, 2347–2354.
28 N. T. N. Phan, X. Li and A. G. Ewing, *Nat. Rev. Chem.*, 2017, **1**, 0048.
29 D. M. Omiatek, Y. Dong, M. L. Heien and A. G. Ewing, *ACS Chem. Neurosci.*, 2010, **1**, 234–245.
30 Y. Jiang, R. Wei, K. Tang, Z. Wang and N. Tan, *J. Ginseng Res.*, 2022, 177.
31 Z. Liu, M. Zhao, Y. Zhang, J. Xue and N. Chen, *Brain Res.*, 2010, **1333**, 1–8.
32 S. Bardo, M. G. Cavazzini and N. Emptage, *Trends Pharmacol. Sci.*, 2006, **27**, 78–84.
33 L. K. Kaczmarek, *Trends Neurosci.*, 1987, **10**, 30–34.
34 D. A. Snyder, M. L. Kelly and D. J. Woodbury, *Cell Biochem. Biophys.*, 2006, **45**, 111–123.

